



Fuel Element Combustion Properties for Live Wildland Utah Shrubs

Chen Shen & Thomas H. Fletcher

To cite this article: Chen Shen & Thomas H. Fletcher (2015) Fuel Element Combustion Properties for Live Wildland Utah Shrubs, Combustion Science and Technology, 187:3, 428-444, DOI: [10.1080/00102202.2014.950372](https://doi.org/10.1080/00102202.2014.950372)

To link to this article: <http://dx.doi.org/10.1080/00102202.2014.950372>



Accepted online: 08 Aug 2014.



Submit your article to this journal [↗](#)



Article views: 52



View related articles [↗](#)



View Crossmark data [↗](#)

FUEL ELEMENT COMBUSTION PROPERTIES FOR LIVE WILDLAND UTAH SHRUBS

Chen Shen and Thomas H. Fletcher

Department of Chemical Engineering, Brigham Young University,
Provo, Utah, USA

*Current field models for wildfire prediction are mostly based on dry or low-moisture fuel combustion research. To better study the live fuel combustion behavior, a laminar flow flat-flame burner was used to provide a convection heating source to ignite an individual live fuel sample. In this research project, four Utah species were studied: Gambel oak (*Quercus gambelii*), canyon maple (*Acer grandidentatum*), big sagebrush (*Artemisia tridentata*), and Utah juniper (*Juniperus osteosperma*). Leaf geometrical parameters measured included individual leaf total mass, thickness, leaf width, leaf length, and moisture content. Time-stamped images of combustion behavior along with time-dependent mass data were recorded via a LabVIEW system. Combustion characteristics were determined by an automated MATLAB routine modified for analyzing Utah species images of burning fuel samples, including time to ignition, time of flame duration, time to maximum flame height, time to burnout, and maximum flame height. Qualitative results included various combustion phenomena like bursting, brand formation, and bending. Sparks accompanied with leaf material bursting out were observed for Utah juniper sample combustion mostly before ignition, especially for segments cut from the top of the branch. Quantitative results included exploration of the best prediction equations for leaf geometrical properties and combustion characteristics. A beta distribution was used to predict the distribution of dry mass. Multiple linear regressions were performed on other leaf geometrical properties and combustion characteristics. Minimized Bayesian information criterion (BIC) value models were achieved by stepwise regression analysis and compared to the previous empirical prediction models.*

Keywords: Combustion; Ignition; Utah shrubs

INTRODUCTION

In order to improve the suppression of wildfires (unwanted and uncontrolled) and the prediction of prescribed fire (ignited intentionally to decrease the amount of live and dead fuel accumulation in a forest), it is important to better understand wildland fire propagation (USDA/USDI, 2005). Weber (1991) and Sullivan (2009a, 2009b, 2009c) performed comprehensive reviews of wildfire modeling and classified types of fire propagation models. The Rothermel model (1972) is a semi-empirical model for a limited number of live and dead fuels that was further developed into wildfire field operational models: FARSITE (Finney, 1998) and BEHAVE (Andrews, 1986). Moreover, some computational

Received 5 February 2014; revised 21 July 2014; accepted 28 July 2014.

Address correspondence to Thomas H. Fletcher, Chemical Engineering Department, Brigham Young University, 350 Clyde Building, Provo, UT 84602, USA. E-mail: tom_fletcher@byu.edu

Color versions of one or more of the figures in the article can be found online at www.tandfonline.com/gcst.

fluid dynamic (CFD) models for wildfire modeling have been developed, such as FIRETEC and WFDS (Clark et al., 2010; Linn, 1997; Mell et al., 2006). Besides CFD models and the Rothermel model (1972), many other wildland fire propagation models were developed based largely on experimental data from dead or dry fuel beds, which might be inappropriate for predicting live wildland fuel combustion, especially at high moisture content (Fletcher et al., 2007; Pickett, 2008). There is a need for better methods to simulate combustion of live wildland fuels, especially for shrubs. Various kinds of live fuel combustion experimental studies have been conducted previously (Dimitrakopoulos and Papaioannou, 2001; Pickett, 2008; Pickett et al., 2010; Smith, 2005; Weise et al., 2005).

More than 2200 combustion experiments were previously conducted on single live fuel samples of various species common in California and Utah (Engstrom et al., 2004; Fletcher et al., 2007; Pickett, 2008; Smith, 2005) over a 3×7.5 cm flat-flame burner (FFB) with no glass cage above to prevent indraft air flow. Both Smith (2005) and Pickett (2008) performed combustion experiments on four fuels from Utah (canyon maple, Gambel oak, big sagebrush, and Utah juniper) and developed empirical correlations for combustion characteristics based on properties of leaves. Different correlations were made for each leaf property. Pickett (2008) developed a first-generation 2D model of Manzanita shrub combustion, based on empirical correlations developed from single leaf experiments. This bush model was capable of predicting overall burn times and amount of fuel unburned. This model was later extended to three dimensions (Prince et al., 2010), including effects of flame coalescence and the effects of wind on flame angle and size, based on the findings of Cole et al. (2011). Model development is still in progress (Prince, 2014), with a need to treat more species and environmental factors. Each leaf is treated independently and compared to the position of other leaves, avoiding the use of a discretized grid. This semi-empirical model may lead to improvements in operational field-scale models. In this work, improved geometrical and combustion data for Utah shrubs were obtained and used to develop improved statistical correlations for subsequent use in shrub combustion simulations.

METHODS

Experimental Apparatus

A flat-flame burner (FFB) was used as the heat source, which can be moved directly under the leaf (see Figure 1). Fuel gases (CH_4 and H_2) and oxidizer (air) were premixed and introduced into the FFB, providing a 1-mm-thick flame at a height of 1 mm above the sintered bronze burner surface. The vertical distance between the FFB and the leaves was typically 5 cm, a point where the gas temperature was 1200 K. This premixed FFB surface was 19 cm \times 25 cm. A cage with glass panels was placed above the FFB to avoid indraft of surrounding air, which introduced natural convection flow recirculation, leading to a decreased effective flame area. This glass cage ensured a uniform concentration of 10 mol% O_2 in the post-flame gases and a laminar flow environment. The horizontal temperature and oxygen profiles in this system were much more uniform than in previous experiments (Fletcher et al., 2007; Pickett, 2008; Smith, 2005) performed with a smaller burner. The live fuel sample (leaf or twig) was placed horizontally or vertically, according to experimental purpose, on a rod connected to a mass balance. Leaf samples were clamped at the stem. Horizontal leaf placement is defined as the leaf pointing horizontally and vertical leaf placement means leaf pointing up. The FFB was placed on a cart, which could be pulled and stopped exactly under the sample.

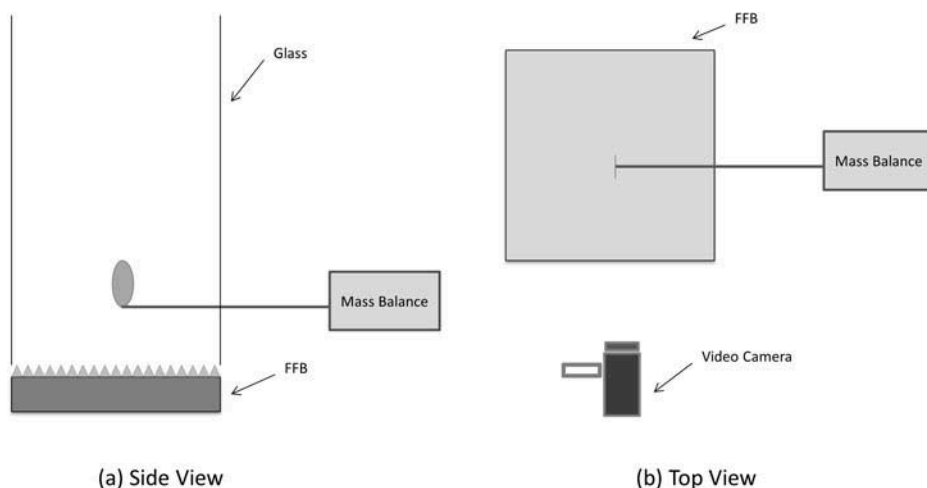


Figure 1 Flat-flame burner experimental set-up.

A bare fine-wire type-K (chromel-alumel) thermocouple was used to measure the gas temperature close to the leaf sample during each experimental run. The bead diameter of the thermocouple was $76\ \mu\text{m}$ and the length was $30.5\ \text{cm}$. A Sony CCD-TRV138 camcorder or a Panasonic SDR-S50P digital camcorder was used to record video images. The images were collected and digitized by a National Instruments PCI-1411 IMAQ device. A National Instruments LabVIEW 7.1 program was used for data collection, which simplified data collection and minimized human error. Video images, temperature, and mass data (from a Mettler Toledo XS204 analytical mass balance) were collected simultaneously with a time-stamp at 18 Hz. Video images were digitized and stored as jpeg files along with the datasheets for each experimental run.

Previously, a CompuTrac moisture analyzer was used to measure the moisture content (MC) of each sample on a dry mass basis. Moisture content in the forest products industry is defined on a dry basis (m_{H_2O}/m_{dry}) (Fletcher et al., 2007; Pickett et al., 2010). Values of MC were measured before and after the combustion experiments, and the two values were averaged together to provide an average MC for all of the experimental runs. However, in this work, a new method was used to better measure and represent the moisture content of samples. The moisture content was determined after every third sample was burned in the FFB. The initial total single leaf mass (m_0) of each of the four samples was measured by a Mettler Toledo AB104 mass balance prior to running the experiment. Then MC can be calculated from:

$$MC = \frac{m_{H_2O}}{m_{dry}} = \frac{m_0 - m_{dry}}{m_{dry}} \quad (1)$$

where m_{H_2O} is the leaf moisture mass.

Leaf length (L) and width (W) were measured with a ruler to an accuracy of $0.1\ \text{mm}$ for each sample prior to each experimental run. Length was defined as the longest distance from tip to stem of a leaf sample. Width was defined as the widest distance from side to side of a leaf sample. Thickness (Δx) was determined by a Chicago brand digital caliper



Figure 2 Images of Utah species individual samples.

with an accuracy of 0.01 mm. Thickness was measured at different positions of the sample (excluding leaf vein) and determined by taking an average of all measurements. For non-broadleaf samples, measurement of the diameter was treated as equivalent to thickness.

Experimental Fuels

Experiments were performed on four kinds of Utah species shown in Figure 2: Gambel oak (*Quercus gambelii* Nutt.), canyon maple (*Acer grandidentatum* Nutt.), big sagebrush (*Artemisia tridentate* Nutt.), and Utah juniper (*Juniperus osteosperma* (Torr.) Little). The samples of Gambel oak, canyon maple, and big sagebrush were primarily collected from Rock Canyon, Provo, Utah. Utah juniper samples were collected from Diamond Fork Canyon near Spanish Fork, Utah. Samples were selected and detached from the branches at random. Samples were collected and burned within five days and are referred to as live fuels. Combustion experiments were performed on live samples with various moisture contents. If combustion testing was not on the collection day, samples were kept moist by watering the stems until testing began.

RESULTS AND DISCUSSION

Qualitative Results

Qualitative results are summarized in this section, including ignition and combustion behavior. Some of the qualitative results for the same species with horizontal placement are consistent with findings from the small FFB from previous research efforts (Fletcher et al., 2007; Pickett, 2008; Smith, 2005).

Ignition behavior. Because of the shape of the Gambel oak leaves, ignition normally started at the tips of the samples when they were placed horizontally. Ignition was observed at multiple tips on the leaf, and would eventually merge into a sustainable flame. On the other hand, for vertical leaf placement, the ignition normally started from the bottom edge closest to the FFB. Generally, these bottom edge ignition flames were intense enough to sustain and propagate towards the center of the leaf. The canyon maple leaf sample mostly ignited from the bottom big saw-tooth tip or edge when placed vertically. The horizontal-placed canyon maple sample showed random local ignition sites on the saw-tooth tips. Utah juniper was burned as a segment (shown as Figure 2c) and ignition occurred at different tips of the small needles. These small flames with local ignition eventually

merged into a sustainable flame and engulfed the entire sample. Big sagebrush samples ignited from the trident tip of the leaf for both single leaf combustion runs and segment (shown as Figure 2d) combustion runs. Sagebrush segment samples ignited more easily than single leaf samples, which could be explained by larger surface area per volume of fuel element exposed to the convective gases.

Combustion behavior. Leaf bending was observed for most of the broadleaf (Gambel oak and canyon maple) sample runs with horizontal or vertical placements and combustion of big sagebrush as well. Figure 3 is an example of bending behavior for Gambel oak burning when the sample was placed horizontally. The square indicates the clamp position where the bottom of the leaf was placed. The curve is showing the bending leaf and the triangle indicates the top of the leaf. The sample bent towards the burner against the convective heating gas flow until maximum flame height was achieved (shown as Figures 3a–3d). Flame height is defined as the distance between the lowest tip of the flame (bright pixel) attached to the sample and the top of the flame (bright pixel) recognized by the video image. The sample bent backwards till its original horizontal placement (shown as Figures 3e–3g).

Brand formation was also observed during four Utah species sample combustion. Figures 3g and 3h show that the sample was eventually detached from the clip as a brand. After pyrolysis, the portion touching the clip was not able to hold the whole leaf sample, which was also often observed for combustion of the canyon maple sample. In some runs,

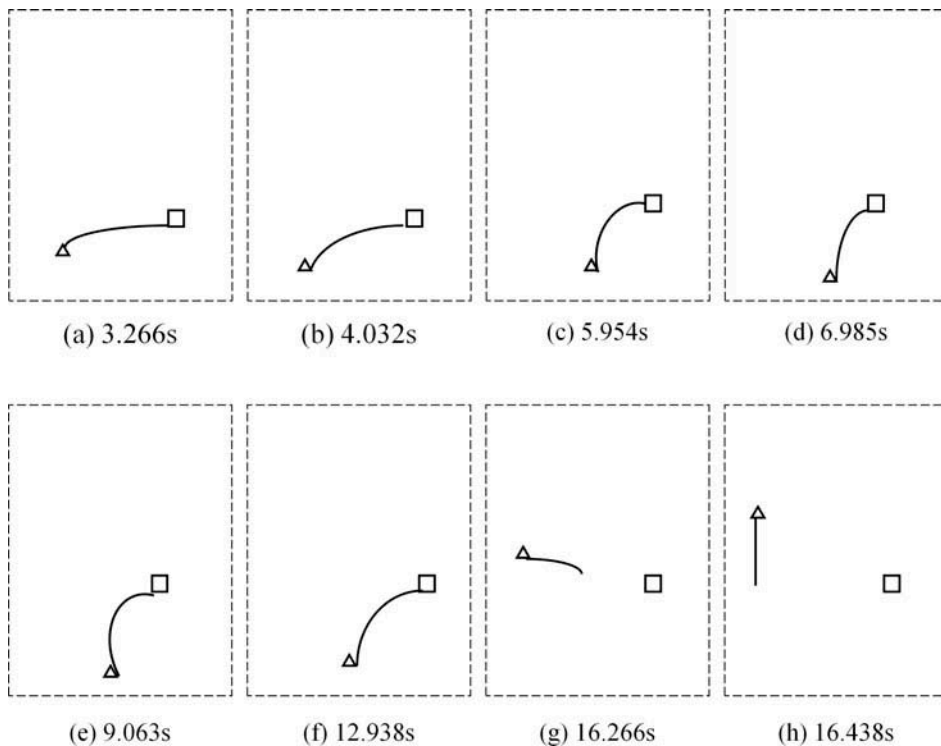


Figure 3 Bending behavior of Gambel oak sample placed vertically. The yellow line shows the leaf orientation. Numbers indicate the time stamp from the initial time of the experimental run.

the stem or part of the leaf that was being held by the clamp burned out, which resulted in the whole sample detaching from the clamp.

Sparks were often observed before the complete ignition of the sample (shown in Shen (2013) as consecutive frames). These pictures showed that the sparks appeared on one frame and disappeared suddenly in the next frame. Accompanying the sparks, there were usually small amounts of leaf material ejected. The sparking behavior was always observed for the segments cut from the top section of a juniper branch. Characteristics identified for the top section of juniper included lighter surface color and thorny surface structure.

Quantitative Results

Approximately 2200 experiments were performed with leaves and fuel segments suspended over the premixed FFB burner with the glass cage present to minimize air in draft. Results from these new experiments are discussed below.

Leaf properties. For this work, a single leaf was the unit sample for the broadleaf species (Gambel oak and canyon maple) and small segments were used for the non-broadleaf species (Utah juniper and big sagebrush). Measurements of leaf properties are summarized in Table 1.

Single leaf dry mass (m_{dry}), leaf thickness (Δx), leaf width (W), and leaf length (L) were cross-correlated to obtain a distribution of physical leaf parameters from experimental measurements. The order of prediction for each leaf parameter is shown in Figure 4, meaning that Δx can depend on m_{dry} , W can depend on both m_{dry} and Δx , etc.

The total single leaf mass (m_0) was measured for each sample before the experiment run. Moisture content (MC) was also estimated for each sample by measurements on representative samples. Hence, single leaf dry mass (m_{dry} , in gram) can be calculated from:

$$m_{dry} = \frac{m_0}{MC + 1} \quad (2)$$

It was found that m_{dry} was well-represented by a beta distribution for most kinds of species studied and, hence, a beta distribution of m_{dry} was utilized as a basis for predicting all other leaf parameters. The goodness of the beta distribution fit of m_{dry} is shown in Figure 5 by the red solid curves, where m_{dry} was normalized as shown in Eq. (3):

Table 1 Measured leaf properties

Species	Moisture content (%)	Single leaf mass (g)	Leaf thickness (mm)	Leaf width (cm)	Leaf length (cm)
Gambel oak	8–138	0.03–1.44	0.11–0.42	1.5–11.8	2.7–14.1
Canyon maple	18–150	0.04–0.92	0.06–0.25	2.7–12.1	2.3–8.7
Utah juniper	33–122	0.06–0.48	0.98–1.90 ^b	NA	1.2–4.5 ^a
Big sagebrush	41–248	0.06–0.86	0.15–0.58	0.3–1.2	2.3–8.5 ^a

^aMeasured as segment length.

^bMeasured as needle diameter.

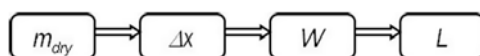


Figure 4 Flowchart illustrating the order of calculation of leaf physical parameters.

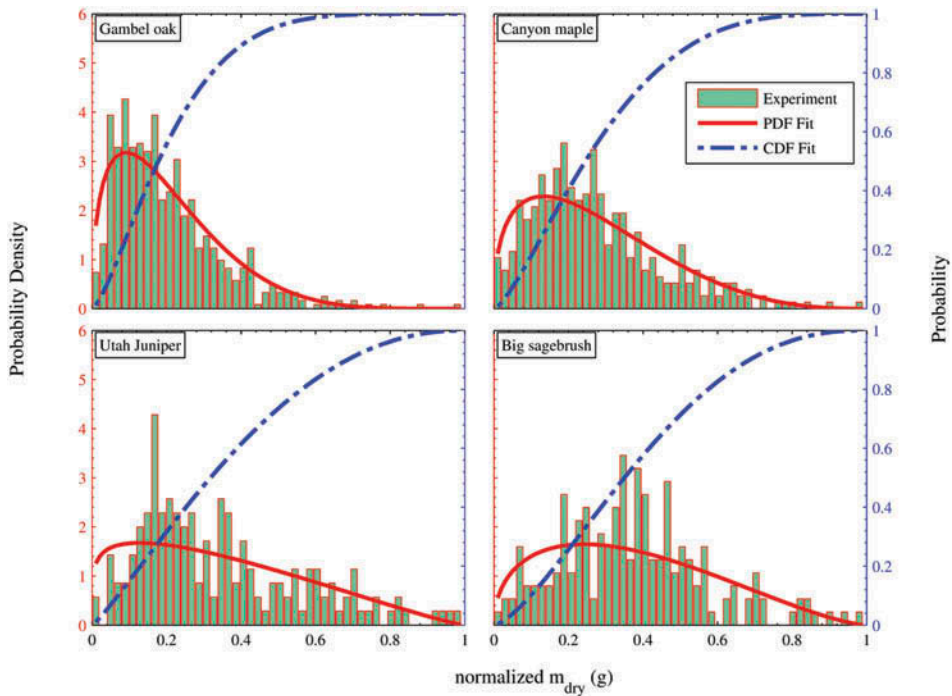


Figure 5 Histogram of the normalized experimental leaf dry mass vs. the fit to a beta distribution and the corresponding cumulative distribution function.

$$\hat{m}_{dry} = \frac{m_{dry} - \text{Min}(m_{dry})}{\text{Max}(m_{dry}) - \text{Min}(m_{dry})} \quad (3)$$

and \hat{m}_{dry} is normalized from m_{dry} . The blue dashed curves are the corresponding cumulative density function. The distributions of m_{dry} for the broadleaf species are more skewed than for the other two species, with a peak at a lower value and a longer tail. The parameters of the beta distributions fitted for single leaf dry mass (m_{dry}) of different species are summarized in Table 2.

Using beta distributions for m_{dry} from Table 2 and the logic diagram in Figure 5, further regression with stepwise analysis to minimize the Bayesian information criterion (BIC) values (Schwarz, 1978) was performed to predict Δx , then W , and then L (all in cm). BIC is widely used for linear non-nested model selection. Posada and Buckley (2004) compared

Table 2 Parameters of the beta distributions fitted for single leaf dry mass

Species	α	β
Gambel oak	1.47 ± 0.09	5.64 ± 0.33
Canyon maple	1.42 ± 0.10	3.72 ± 0.31
Utah juniper	1.17 ± 0.12	2.18 ± 0.28
Big sagebrush	1.47 ± 0.12	2.46 ± 0.31

Note: \pm indicates the 95% confidence interval.

Table 3 Summary of regression analysis on leaf geometrical properties for Utah species

Species	Predictive equation	MSE	R ²
Gambel oak	$\Delta x = 0.27 + 0.052 \cdot MC + 0.035 \cdot Ln(m_{dry})$	0.0012	0.35
	$W = 3.51 - 7.68 \cdot \Delta x + 11.96 \cdot m_{dry} + 3.76 \cdot m_{H2O}$	0.63	0.73
	$L = 10.16 + 0.26 \cdot W + 1.56 \cdot Ln(m_{dry}) + 0.50 \cdot Ln(m_{H2O})$	0.76	0.77
Canyon maple	$\Delta x = 0.067 + 0.046 \cdot MC + 0.21 \cdot m_{dry}$	0.0006	0.37
	$W = 11.72 - 0.81 \cdot MC - 10.66 \cdot \Delta x + 9.51 \cdot m_{dry} + 1.67 \cdot Ln(m_{H2O})$	0.45	0.81
	$L = 6.82 - 1.19 \cdot MC + 0.30 \cdot W + 1.01 \cdot Ln(m_{H2O})$	0.37	0.74
Utah juniper	$\Delta x = 0.88 + 0.50 \cdot MC + 0.62 \cdot m_{dry}$	0.033	0.21
	$L = 5.54 + 1.01 \cdot Ln(m_{dry})$	0.21	0.46
Big sagebrush	$\Delta x = 0.24 + 0.59 \cdot m_{dry}$	0.0043	0.14
	$L = 5.54 - 4.92 \cdot \Delta x + 8.66 \cdot m_{H2O}$	0.72	0.49

different model selection methods and pointed out that BIC tends to select simpler models than Akaike Information Criterion (AIC) and Bayesian factors. The resulting correlations from the BIC analysis technique are shown in Table 3. These forms of equations were compared to forms of equations suggested in a semi-empirical bush model (Prince et al., 2010). Because of the better goodness of fit, smaller mean-square error (MSE) values compared to the values of regression results from previous equation forms (more details addressed in Shen (2013)), the equations in Table 3 for Gambel oak, Canyon maple, and Utah juniper are recommended to be used for leaf property predictions.

The apparent dry density of a leaf (ρ_{leaf}) is defined as the dry mass of a single leaf divided by the leaf volume, as shown in Eq. (4). Leaf volume is approximated as the smallest volume of a rectangular that can contain the leaf. Values of ρ_{leaf} were calculated for broadleaf species (Gambel oak and canyon maple), which is regarded as a possible term for the stepwise regression of combustion characteristics shown in the next section. A leaf-shape dependent void fraction factor could be added, but this effect would be automatically incorporated into the coefficient in the regression for ρ_{leaf} .

$$\rho_{leaf} = \frac{m_{dry}}{L \cdot W \cdot \Delta x} \tag{4}$$

Combustion characteristics. Combustion characteristics were determined by custom automated MATLAB codes (Prince, 2014; Shen, 2013) to process the time-stamped video images. These combustion characteristics included time to ignition (t_{ig} , in s), time to maximum flame height (t_{fh} , in s), time of flame duration (t_{fd} , in s), maximum flame height ($h_{f,max}$, in cm), etc. Time to ignition (t_{ig}) is defined as the time difference between exposure to heat flux and ignition. The time of flame duration (t_{fd}) is the time difference between the moment of ignition and the moment of burnout. The flame height for each frame during combustion of each live fuel sample was determined as the vertical distance from the bottom bright pixel to the top bright pixel and the maximum flame height ($h_{f,max}$) was chosen among these frames. A brightness threshold could be adjusted to ensure that the visual flame height was captured from the video images. The time to maximum flame height (t_{fh}) was defined as the amount of time between the moment of exposure to heat flux and the moment of reaching the maximum flame height. Combustion characteristics measurements are summarized in Table 4. It was observed that t_{ig} and t_{fh} varied significantly between

Table 4 Measured combustion characteristics

Sample orientation	Gambel oak		Canyon maple		Utah juniper		Big sagebrush	
	Horizontal	Vertical	Horizontal	Vertical	Horizontal	Vertical	Horizontal	Vertical
Time to ignition (t_{ig} , s)	1.45 ± 0.13	2.68 ± 0.28	0.84 ± 0.10	1.12 ± 0.13	3.94 ± 0.24	4.55 ± 0.39	1.26 ± 0.45	2.19 ± 0.29
Difference ^a	85%		33%		15%		74%	
Time to maximum flame height (t_{fh} , s)	4.15 ± 0.25	7.13 ± 0.45	2.14 ± 0.19	6.06 ± 0.32	6.17 ± 0.47	8.08 ± 0.95	2.89 ± 0.78	9.17 ± 0.84
Difference	72%		183%		31%		217%	
Time of flame duration (t_{fd} , s)	6.35 ± 0.42	9.10 ± 0.51	4.85 ± 0.31	4.88 ± 0.24	14.55 ± 0.86	14.71 ± 0.81	14.78 ± 2.65	10.11 ± 1.21
Difference	43%		1%		1%		32%	
Maximum flame height ($t_{f,max}$, cm)	19.60 ± 1.02	16.72 ± 0.82	18.00 ± 1.30	16.35 ± 1.03	8.93 ± 0.61	6.78 ± 0.46	14.00 ± 1.21	11.04 ± 0.88
Difference	15%		9%		24%		21%	

Note: Values are listed as the mean ± the 95% confidence interval.

^aThis is the relative percentage difference from the horizontal value.

Table 5 Comparison of average combustion characteristics data for horizontal leaf placement

	Species	Pickett (2008)	This work
t_{ig}	Gambel oak	0.71 ± 0.07	1.45 ± 0.13
	Canyon Maple	0.64 ± 0.10	0.84 ± 0.10
	Utah juniper	1.45 ± 0.24	3.94 ± 0.24
t_{fn}	Gambel oak	3.01 ± 0.26	4.15 ± 0.25
	Canyon Maple	3.82 ± 0.27	2.14 ± 0.19
	Utah juniper	8.06 ± 0.68	6.17 ± 0.47
t_{fd}	Gambel oak	6.32 ± 0.27	6.35 ± 0.42
	Canyon Maple	5.77 ± 0.27	4.85 ± 0.31
	Utah juniper	21.08 ± 1.91	14.55 ± 0.86
$h_{f,max}$	Gambel oak	6.7 ± 0.4	19.60 ± 1.02
	Canyon Maple	5.3 ± 0.3	18.00 ± 1.30
	Utah juniper	8.0 ± 0.5	8.93 ± 0.61

horizontal and vertical sample placement. One of the explanations can be the large temperature gradient in vertically-placed leaf sample, which delayed sample ignition. However, t_{fd} and $h_{f,max}$ were not affected as significantly as t_{ig} and t_{fn} , which suggested orientation would have less influence on flame propagation.

The data for horizontal leaf placement were compared to the data reported by Pickett (2008) as shown in Table 5. It was noticed that t_{ig} and $h_{f,max}$ were larger in this work, which can be explained by the increasing surface area of FFB and glass cage installed to prevent the indraft air and to ensure the 10 mol% oxygen content near the sample.

Leaves with a thickness less than 1 mm are usually regarded as thermally thin (Brabauskas, 2003), indicating a linear relationship between time to ignition (t_{ig}) and leaf thickness (Δx). Only the Δx of juniper was larger than 1 mm among these four species. The t_{ig} data are very scattered, which increased the difficulty to developing a general correlation on t_{ig} . Linear regressions on t_{ig} versus Δx are shown in Figure 6. The blue straight lines are mean values of t_{ig} . The linear regression coefficients and comparisons to the fits by means are shown in Table 6. The MSE using a mean value was similar to the MSE using a linear correlation based on Δx . This indicates that the correlation with Δx is weak. Hence, whether these live fuel samples can be treated as thermally thin is still unclear. Moreover, significant horizontal temperature gradients were measured on the leaf surface (Pickett, 2008; Pickett et al., 2010; Prince and Fletcher, 2014).

Time to ignition (t_{ig}) was also expected to correlate with leaf moisture mass (m_{H_2O}) (Mardini and Lavine, 1995; Moghtaderi et al., 1997; Montgomery and Cheo, 1969; Pickett, 2008; Smith, 2005; Weise et al., 2005; Xanthopoulos and Wakimoto, 1993). Catchpole et al. (2002) also suggested that evaporated moisture might dilute the volatile gases and cause the t_{ig} to increase. Linear regressions are shown in Figure 7 and Table 7. Based on these results, it is also hard to draw a significant conclusion that t_{ig} is correlated with m_{H_2O} . Thus, further regression analysis is necessary to study the prediction equations for t_{ig} by including more potential leaf property variables for the regression analysis.

Time of flame duration (t_{fd}) was correlated with m_{dry} as shown in Figure 8 and Table 8. It was observed that the slopes for linear regression of t_{fd} versus m_{dry} were nonzero for these species, which indicated a better correlation than just represented by the mean. It is obvious that the t_{fd} is larger for juniper segments than Gambel oak and maple leaves for similar values of m_{dry} . The slope of the juniper correlation is also much larger than that of Gambel

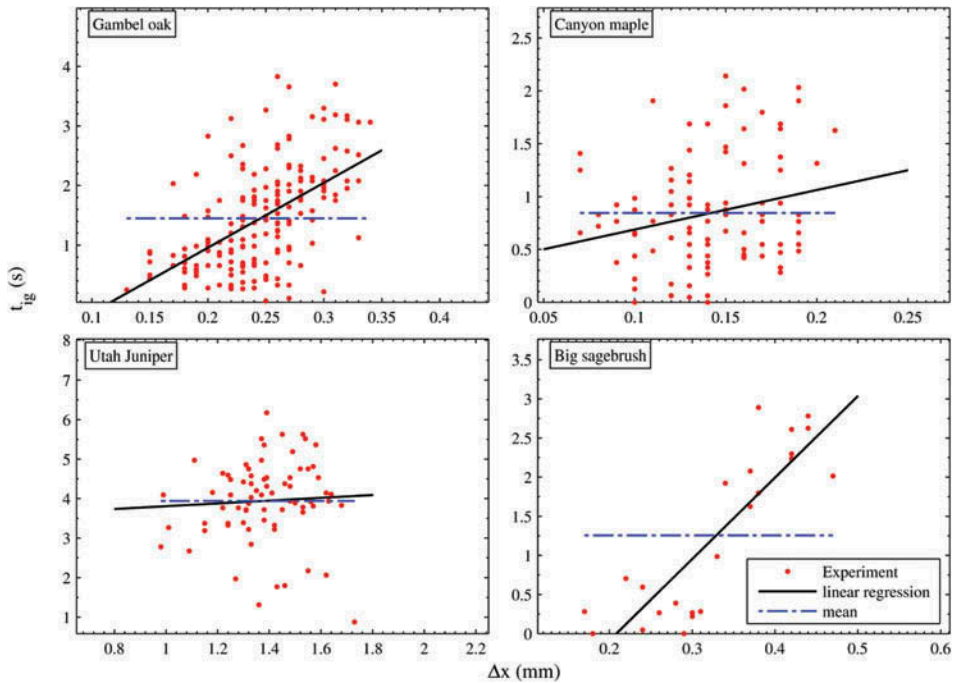


Figure 6 Time to ignition vs. leaf thickness for Gambel oak, canyon maple, Utah juniper, and big sagebrush.

Table 6 Summary of linear regressions for time to ignition vs. leaf thickness

Species	Linear regression			Fit by mean	
	Intercept	Slope	MSE	Mean	MSE
Gambel oak	-1.22 ± 0.61	10.89 ± 2.45	0.52	1.45 ± 0.13	0.74
Canyon maple	0.31 ± 0.45	3.74 ± 3.10	0.26	0.84 ± 0.10	0.27
Utah juniper	3.45 ± 2.11	0.35 ± 1.52	1.08	3.94 ± 0.24	1.05
Big sagebrush	-2.17 ± 0.95	10.41 ± 2.79	0.30	1.26 ± 0.45	1.04

Note: Values are listed as the mean \pm the 95% confidence interval.

oak and maple. Nevertheless, it is still necessary to perform further multi-linear regression analysis on t_{fd} since other independent variables may also be important. For example, the variables that can describe the interior structure of leaves might contribute to the predictions of volatile release, which will lead to better correlation forms for t_{fd} .

It was also expected that $h_{f,max}$ would linearly correlate with m_{dry} . This linear relationship was also explored and the results (Figure 9 and Table 9) indicated that the slopes were significant for all the species except big sagebrush. It is noticed that the range of juniper data is narrower due to the smaller and more consistent segment size. The Gambel oak data seem to be scattered evenly about the linear correlation. However, the scatter in the maple data seems to increase at higher values of m_{dry} . The scatter implies that other leaf properties may have effects on $h_{f,max}$.

Because the goodness of fit for these basic linear regression analyses is poor to some extent, it is necessary to perform multiple linear regressions. A stepwise regression

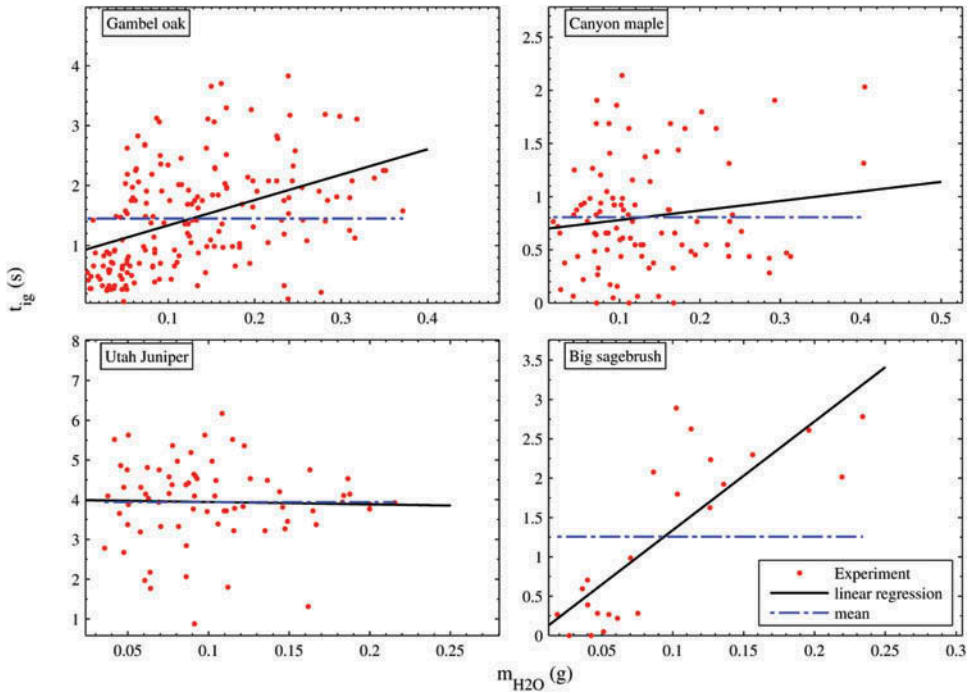


Figure 7 Time to ignition vs. leaf moisture mass for Gambel oak, canyon maple, Utah juniper, and big sagebrush.

Table 7 Summary of linear regressions for time to ignition vs. leaf moisture mass

Species	Linear regression			Fit by mean	
	Intercept	Slope	MSE	Mean	MSE
Gambel oak	0.91 ± 0.20	4.23 ± 1.31	0.61	1.45 ± 0.13	0.74
Canyon maple	0.68 ± 0.20	0.90 ± 1.28	0.26	0.84 ± 0.10	0.26
Utah juniper	4.00 ± 0.60	-0.60 ± 5.44	1.08	3.94 ± 0.24	1.05
Big sagebrush	-0.04 ± 0.50	13.82 ± 4.44	0.38	1.26 ± 0.45	1.04

Note: Values are listed as the mean \pm the 95% confidence interval.

with bidirectional elimination was used to achieve the statistically best models based on Bayesian information criterion (BIC). This procedure takes all the possible leaf properties (MC , W , L , Δx , m_{dry} , m_{H2O} , and ρ_{leaf}) into account, which were obtained from experimental measurements. The best statistical models recommended are shown in Table 10. The number of big sagebrush data was believed to be too small to be statistically relevant and, hence, sagebrush correlations are not included here. Further experiments on big sagebrush segments are necessary. As shown in Table 10, the MSEs for the BIC correlations are smaller than those for the linear regression shown previously. Note that the correlations for each species do not use the same variables and, hence, are not general in nature (i.e., the correlations cannot be applied to other species). Although the R^2 values are quite low for some correlations, indicating more independent variables needed for regression, it is

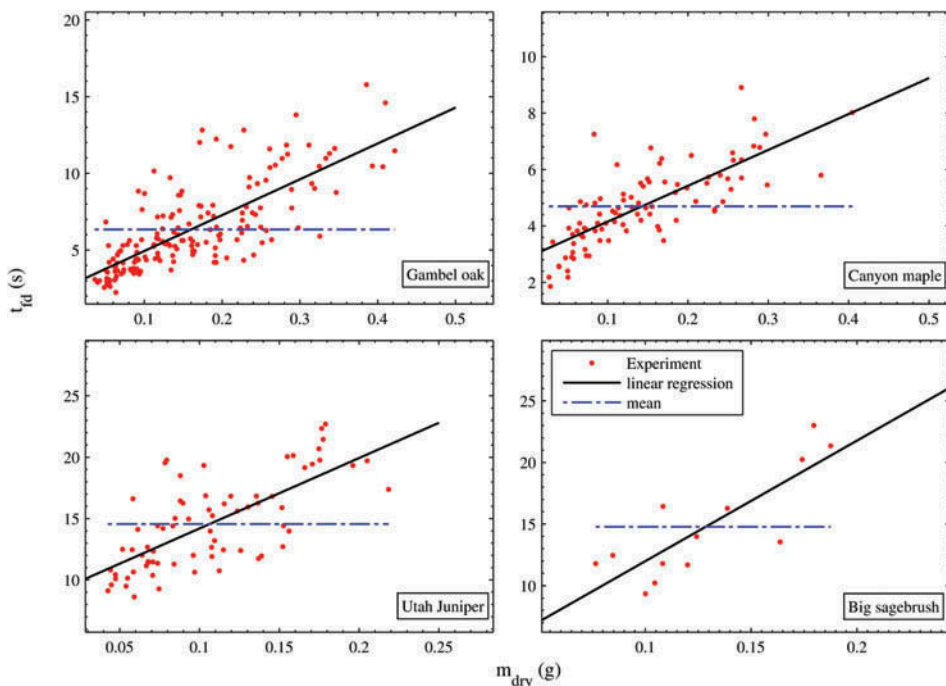


Figure 8 Time of flame duration vs. leaf volatile mass for Gambel oak, canyon maple, Utah juniper, and big sagebrush.

Table 8 Summary of linear regressions for the time of flame duration versus leaf dry mass

Species	Linear regression			Fit by mean	
	Intercept	Slope	MSE	Mean	MSE
Gambel oak	2.60 ± 0.57	23.38 ± 3.11	3.36	6.35 ± 0.42	7.73
Canyon maple	2.88 ± 0.37	12.71 ± 2.24	0.80	4.85 ± 0.31	1.89
Utah juniper	8.46 ± 1.59	57.38 ± 13.84	6.82	14.55 ± 0.86	13.11
Big sagebrush	2.21 ± 5.92	97.77 ± 44.36	6.68	14.78 ± 2.65	17.75

Note: Values are listed as the mean \pm the 95% confidence interval.

believed that these correlations of combustion characteristics are the best available for live leaves or segments for these species.

SUMMARY

Observations of combustion experiments of live leaves showed that ignition was initiated at the tip or edge of the leaf, where local surface area was relatively large. Bending behavior was observed during combustion experiments of Gambel oak, canyon maple, and big sagebrush. Brand formation was mainly observed in combustion of leaf samples of light weight. Some samples detached from the clip after burnout and some samples detached from the clip when samples were still flaming, especially for canyon maple. Sparks and

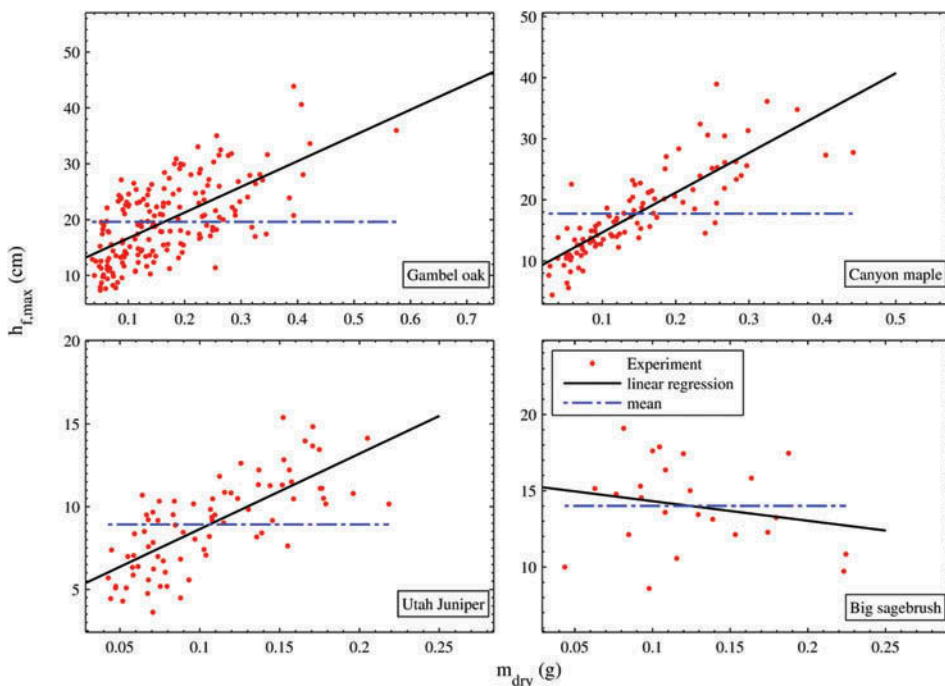


Figure 9 Maximum flame height vs. leaf volatile mass for Gambel oak, canyon maple, Utah juniper, and big sagebrush.

Table 9 Summary of linear regressions for the maximum flame height vs. leaf dry mass

Species	Linear regression			Fit by mean	
	Intercept	Slope	MSE	Mean	MSE
Gambel oak	12.07 ± 1.58	45.99 ± 8.33	29.25	19.60 ± 1.02	48.10
Canyon maple	8.15 ± 1.50	65.16 ± 8.74	15.03	18.00 ± 1.30	47.60
Utah juniper	4.08 ± 1.08	45.61 ± 9.34	3.42	8.93 ± 0.61	7.42
Big sagebrush	15.60 ± 3.45	-12.84 ± 25.95	8.19	14.00 ± 1.21	7.87

Note: Values are listed as the mean ± the 95% confidence interval.

bursting behavior were observed usually before ignition of the Utah juniper sample, which occurred particularly for young juniper segments cut from the top of the branch.

Statistical analyses were performed on both leaf geometrical properties and combustion characteristics. A beta distribution was used to describe individual leaf dry mass (m_{dry}). Multiple linear regressions were performed to correlate leaf thickness (Δx), leaf width (W), and leaf length (L) (in this order). Multiple linear regression correlations for combustion characteristics (time to ignition (t_{ig}), time of flame duration (t_{fd}), time to maximum flame height (t_{fh}), time to burnout (t_{brn}), maximum flame height ($h_{f,max}$), etc.) were also developed. Linear regressions for t_{ig} , t_{fd} , and $h_{f,max}$ were developed based on Δx , m_{H2O} , and/or m_{dry} and compared with mean values. Minimized Bayesian information criterion value models were achieved by stepwise regression analysis of several variables. Correlations were first developed based on single properties. The BIC-based correlations

Table 10 Summary of recommended correlations for combustion characteristics for Utah species

Species	Predictive equation	MSE	R ²
Gambel oak	$t_{ig} = -1.15 + 1.59 \cdot MC - 0.094 \cdot W + 7.13 \cdot \Delta x$	0.32	0.58
	$t_{fd} = 3.05 + 1.02 \cdot \ln(MC) + 22.82 \cdot m_{dry}$	3.11	0.61
	$h_{f,max} = 2.24 - 9.15 \cdot MC + 2.04 \cdot W + 1.54 \cdot L + 24.55 \cdot \Delta x$	15.93	0.65
Canyon maple	$t_{fh} = 3.02 - 0.31 \cdot L + 14.28 \cdot m_{H2O}$	0.61	0.57
	$t_{ig} = 0.92 + 0.86 \cdot \ln(MC)$	0.15	0.40
	$t_{fd} = 1.44 + 12.44 \cdot \Delta x + 6.78 \cdot m_{dry} + 4.49 \cdot m_{H2O}$	0.57	0.71
Utah juniper	$h_{f,max} = -21.55 + 2.68 \cdot W + 1.37 \cdot L + 62.14 \cdot \Delta x - 27.42 \cdot m_{H2O} + 29.72 \cdot \rho_{leaf}$	10.98	0.75
	$t_{fh} = 10.79 + 1.07 \cdot \ln(MC) - 0.54 \cdot W + 2.05 \cdot \ln(m_{dry})$	0.38	0.48
	$t_{ig}^a = -0.60 \cdot m_{H2O} + 4.00$	1.08	0.0007
	$t_{fd} = 5.21 + 3.24 \cdot \Delta x + 53.00 \cdot m_{H2O}$	6.01	0.51
	$h_{f,max} = 5.47 - 4.21 \cdot MC + 1.00 \cdot L + 33.90 \cdot m_{H2O}$	3.58	0.45
	$t_{fh} = 6.23 + 2.75 \cdot \ln(MC) + 14.78 \cdot m_{dry}$	6.41	0.10

^aCorrelation used from single component analysis rather than BIC analysis.

were then developed based on multiple properties, which reduced the mean-square error (MSE) by an average of 25% from that of the single property correlations. Recommended correlations were presented and these species-specific correlations can be embedded into semi-empirical multi-leaf combustion models being developed (Prince et al., 2010).

ACKNOWLEDGMENTS

Any opinions, findings, and conclusions or recommendations expressed in this article are those of the PI and do not necessarily reflect the views of the National Science Foundation; NSF has not approved or endorsed its content. Dallan Prince gave support and suggestions. The following undergraduate students assisted in conducting experiments and data analysis for this project: Jay Liu, Ganesh Bhattarai, Marianne Fletcher, Kenneth Alford, Kelsey Wooley, Eddie Overy, Merete Carpener, Sydney Hansen, Victoria Lansinger, Kristen Nicholes, and Kellen Mecham.

FUNDING

This research was funded in part by the National Science Foundation Grant CBET-0932842.

REFERENCES

- Andrews, P.L. 1986. Behave: Fire behavior prediction and fuel modeling system—Burn subsystem, Part 1. General Technical Report INT-194. USDA Forest Service.
- Brabauskas, V. 2003. *Ignition Handbook*, Fire Science Publishers, Issaquah, WA.
- Catchpole, W.R., Catchpole, E.A., Tate, A.G., Butler, B.W., and Rothermel, R.C. 2002. *A Model for the Steady Spread of Fire through a Homogeneous Fuel Bed*, Millpress, Rotterdam, Netherlands.
- Clark, M.M., Fletcher, T.H., and Linn, R.R. 2010. A sub-grid, mixture-fraction-based thermodynamic equilibrium model for gas phase combustion in Firetec: Development and results. *Int. J. Wildland Fire*, **19**(2), 202–212.

- Cole, W.J., Dennis, M.H., Fletcher, T.H., and Weise, D.R. 2011. The effects of wind on the flame characteristics of individual leaves. *Int. J. Wildland Fire*, **20**(5), 657–667.
- Dimitrakopoulos, A.P., and Papaioannou, K.K. 2001. Flammability assessment of Mediterranean forest fuels. *Fire Technol.*, **37**(2), 143–152.
- Engstrom, J.D., Butler, J.K., Smith, S.G., Baxter, L.L., T. H. Fletcher, T.H., and Weise, D.R. 2004. Ignition behavior of live California chaparral leaves. *Combust. Sci. Technol.*, **176**, 1577–1591.
- Finney, M.A. 1998. Farsite: Fire area simulator-model development and evaluation. Research Paper RMRS-RP-4. USDA Forest Service.
- Fletcher, T.H., Pickett, B.M., Smith, S.G., Spittle, G.S., Woodhouse, M.M., Haake, E., and Weise, D.R. 2007. Effects of moisture on ignition behavior of moist California chaparral and Utah leaves. *Combust. Sci. Technol.*, **179**, 1183–1203.
- Linn, R.R. 1997. A transport model for prediction of wildfire behavior. PhD. Department of Mechanical Engineering, New Mexico State University, Las Cruces, NM.
- Mardini, J.A., and Lavine, A.S. 1995. Heat and mass transfer in green wood during fires. In *ASME International Mechanical Engineering Congress and Exposition*, San Francisco, CA, November 12–17, ASME, New York, **317-2**, pp. 139–146.
- Mell, W.E., Manzello, S.L., and Maranghides, A. 2006. Numerical modeling of fire spread through trees and shrubs. Presented at the V International Conference on Forest Fire Research, Coimbra, Portugal, November 27–30.
- Moghtaderi, B., Novozhilov, V., Fletcher, D.F., and H. Kent, J.H. 1997. A new correlation for bench-scale piloted ignition data of wood. *Fire Safety J.*, **29**, 41–59.
- Montgomery, K.R., and Cheo, P.C. 1969. Moisture and salt effects on fire retardance in plants. *Am. J. Botany*, **56**(9), 1028–1032.
- Pickett, B.M. 2008. Effects of moisture on combustion of live wildland forest fuels. PhD. thesis, Chemical Engineering Department, Brigham Young University, Provo, Utah.
- Pickett, B.M., Isackson, C., Wunder, R., Fletcher, T.H., Butler, B.W., and Weise, D.R. 2010. Experimental measurements during combustion of moist individual foliage samples. *Int. J. Wildland Fire*, **19**, 1–10.
- Posada, D., and Buckley, T.R. 2004. Model selection and model averaging in phylogenetics: Advantages of Akaike information criterion and Bayesian approaches over likelihood ratio tests. *Syst. Biol.*, **53**(5), 793–808.
- Prince, D.R. 2014. Fire spread in sparse vegetation. PhD dissertation. Chemical Engineering Department, Brigham Young University, Provo, Utah (In Progress).
- Prince, D.R., Andersen, B., Cole, W., Dennis, M., and Fletcher, T.H. 2010. Modeling a burning shrub with and without wind using a semi-empirical model. Presented at the International Association of Wildland Fire 3rd Fire Behavior and Fuels Conference, Spokane, WA, October 25–29.
- Prince, D.R., and Fletcher, T.H. 2014. The fundamental burning behavior of live and dead leaves: 1. Measurements. *Combust. Sci. Technol.*, **186**, 1844–1857.
- Rothermel, R.C. 1972. A mathematical model for predicting fire spread in wildland fuels. Research Paper INT-115. USDA Forest Service.
- Schwarz, G. 1978. Estimating the dimension of a model. *Ann. Statist.*, **6**(2), 461–464.
- Shen, C. 2013. Application of fuel element combustion properties to a semi-empirical flame propagation model for live wildland Utah shrubs. MS thesis. Chemical Engineering Department, Brigham Young University, Provo, Utah.
- Smith, S.G. 2005. Effects of moisture on combustion characteristics of live California chaparral and Utah foliage. MS thesis. Chemical Engineering Department, Brigham Young University, Provo, Utah.
- Sullivan, A.L. 2009a. Wildland surface fire spread modelling, 1990–2007. 1: Physical and quasi-physical models. *Int. J. Wildland Fire*, **18**(4), 349–368.
- Sullivan, A.L. 2009b. Wildland surface fire spread modelling, 1990–2007. 2: Empirical and quasi-empirical models. *Int. J. Wildland Fire*, **18**(4), 369–386.

- Sullivan, A.L. 2009c. Wildland surface fire spread modelling, 1990–2007. 3: Simulation and mathematical analogue models. *Int. J. Wildland Fire*, **18**(4), 387–403.
- USDA/USDI. 2005. Federal fire and aviation operations action plan. F. A. A. M. USDA Forest Service/Department of the Interior.
- Weber, R.O. 1991. Modelling fire spread through fuel beds. *Prog. Energy Combust. Sci.*, **17**(1), 67–82.
- Weise, D.R., White, R.H., Beall, R.C., and Etlinger, M. 2005. Use of the cone calorimeter to detect seasonal differences in selected combustion characteristics of ornamental vegetation. *Int. J. Wildland Fire*, **14**(3), 321–338.
- Xanthopoulos, G., and Wakimoto, R.H. 1993. A time to ignition—Temperature—Moisture relationship for branches of three western conifers. *Can. J. For. Res.*, **23**, 253–258.